EUROPEAN ORGANIZATION FOR NUCLEAR RESEARCH
European Laboratory for Particle Physics

Large Hadron Collider Project

LHC Project Report 516

OPTICAL INVESTIGATIONS OF HEII TWO PHASE FLOW

E. di Muoio[1], B. Jager[1], L. Puech[2], B. Rousset[1], P. Thibault[2], R. van Weelderen[3] and P. E. Wolf [2]

Abstract

The LHC development program relies on cryogenic tests of prototype and model magnets. This vigorous program is pursued in a dedicated test facility based on several vertical cryostats working at superfluid helium temperatures. The performance of the facility is detailed. Goals and test equipment for currently performed studies are reviewed: quench analysis and magnet protection studies, measurement of the field quality, test of ancillary electrical equipment like diodes and busbars. The paper covers the equipment available for tests of prototypes and some special series of LHC magnets to come.

1 DRFMC/SBT/CEAG, Grenoble, France
2 CRTBT/CNRS, Grenoble, France
3 CERN, LHC Division

Presented at the 2001 Cryogenic Engineering Conference and International Cryogenic Materials Conference
CEC/ICMC 2001
16-20 July 2001, Madison, Wisconsin, USA

Administrative Secretariat
LHC Division
CERN
CH - 1211 Geneva 23
Switzerland

Geneva, 19 October 2001

OPTICAL INVESTIGATIONS OF HEII TWO PHASE FLOW

E. di Muoio[1], B. Jager[1], L. Puech[2], B. Rousset[1], P. Thibault[2],

R. van Weelderen[3], P. E. Wolf[2]

[1]DRFMC/SBT/CEAG

Grenoble, 38054, France

[2]CRTBT/CNRS

Grenoble, 38042, France

[3]CERN, European Organization for Nuclear Research, LHC Division,
CH-1211 Geneva, 23, Switzerland

ABSTRACT

We describe the optical techniques we used to detect droplets in the HeII two phase flow of the Cryoloop experiment. These include quantitative light scattering, imaging, and laser phase sensitive anemometry and granulometry (PDPA). We demonstrate that droplets appear for vapor velocities larger than 5 m/s, and that they progressively invade the entire pipe cross section as the vapor velocity is increased. Estimates are given for the droplet size and density.

INTRODUCTION

In the Large Hadron Collider, the superconducting magnets will be cooled by a He II two-phase flow. The purpose of the Cryoloop experiment was to study the heat transfer capabilities provided by such a flow. At large vapor velocities, the first version of the experiment showed an improved heat transfer between the wall of the pipe and the HeII liquid, with respect to a purely stratified situation. The purpose of the second version of the experiment was to explore the origin of this behavior, and to discriminate between two

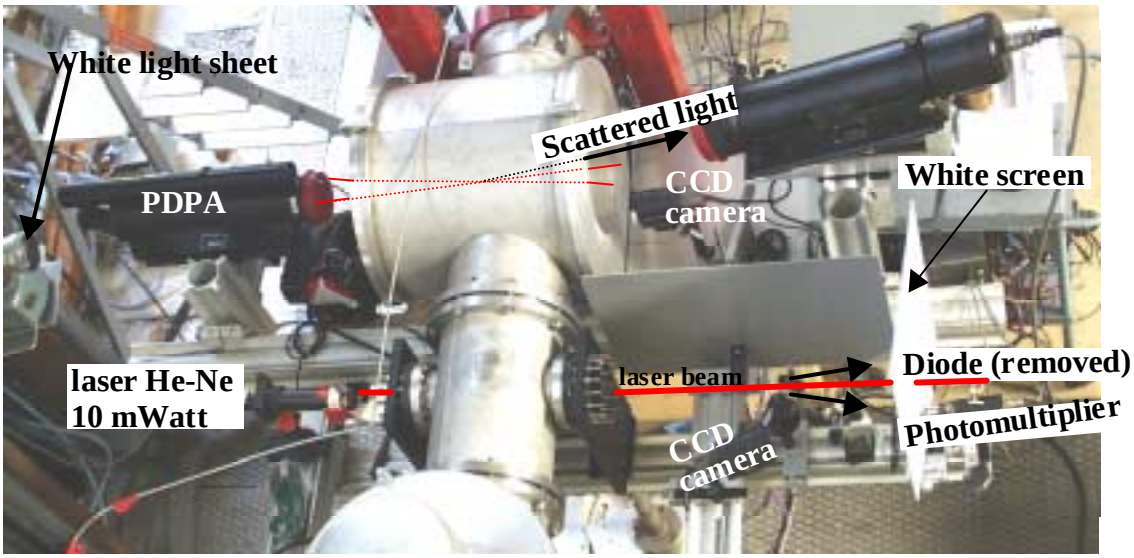

FIGURE 1. picture of the Cryoloop II optical sector

possible mechanisms which both increase the contact area between the wall and the liquid : transition to an annular flow, or apparition of a mist flow. In this paper, we describe the optical techniques we used to detect and characterize the mist flow which, indeed, occurs at large vapor velocities. The analysis of the data, still in progress, should allow us to see whether this phenomenon can account for the improved heat transfer.

EXPERIMENTAL METHODS

Optical ports

The "Cryoloop II" experiment has two optical ports, shown in FIGURE 1. The first one gives access to a portion of the pipe where the tube is made out of Pyrex glass. This allows to visualize the flow over the full pipe cross section, over a 150 mm long portion. We used this access for global imaging, as well as for granulometry and velocity measurements using Particle Phase Doppler Analysis (PDPA). The second port, located downstream, opens to a stainless steel portion of the pipe. To this aim, two 15 mm diameter holes were drilled across an horizontal diameter of the pipe, the leak tightness being made by flat optical windows, whose flanges were soldered onto the outer surface of the tube. The flow disturbance was minimized by sealing the orifices, on the inner surface of the tube, by thin, round, microscope slides. This port was used for quantitative light scattering measurements, as described below.

Light scattering

The primary goal of the experiment was to detect whether droplets were present in the vapor region. To this aim, a horizontal 10 mW He-Ne laser beam was shined through the tube, using the second optical port described above. In order to maximize the detection sensitivity, we monitor the light scattered at small angles (<10°) with respect to the incident direction. Indeed, as soon as the droplets are larger than several microns in diameter, so as to be in the regime of geometrical optics, they scatter light close to the forward direction, due to the very low refractive index of liquid Helium (n=1.025)[2].

Droplets can then be detected either by simple visual inspection, or by collecting the scattering light with some device. In our case, we used three different methods.

First, a white screen was placed at a large distance of the pipe (850 mm as compared to a pipe diameter of 40 mm), and a CCD camera (coupled to a 8 bits frame grabber) was used to capture images of the screen, giving access to the angular dependence of the scattered light.

Second, a 5 mm diameter was drilled into the screen, letting the non scattered beam impinge on a photodiode located behind the screen. The reduction of the photodiode signal (I) when droplets are present is a direct measure of l, the scattering mean free path of light, according to Lambert-Beer's law $I/I_0=\exp(-L/l)$, where L is the tube diameter. Note that the hole serves an essential dual role : without this hole, the first measurement would be flawed by laser light diffusing along the screen from the incidence point of the main beam.

Finally, an other 5 mm diameter hole was drilled at a distance from the first one, corresponding to a scattering angle of about 70 mrad, and the light scattered in this direction was measured with a photomultiplier located behind the hole.

Due to the high sensitivity and short time constant of the photomultiplier, this provided the opportunity to detect individual scatterers. On the other hand, the CCD measurements, while slower (typical exposure time was 1/125 s) and less sensitive (only a small fraction of the light impinging the screen is diffused back onto the CCD), have the unmatched advantage to give the full angular dependence of the average scattered light.

Global imaging and PDPA

With the technique described above, we detect the mist in the middle portion of the tube only. As we can expect strong vertical gradients of the droplets density, these measurements have to be complemented by global imaging. To this aim, we used a sheet of collimated white light to illuminate the glass portion of the pipe along a several millimeters wide slice. The slice was observed under a small angle (approximately 10°) by a second CCD camera. A frontal lens of typical focal length 300 mm was used to image the tube at infinity. This allowed to visualize as well the liquid-gas interface as the clouds of droplets above the interface.

These measurements were complemented by PDPA measurements using a commercial apparatus (Aerometrics). In this technique, two horizontal, coherent, laser beams intercept inside the pipe at a small angle (about 5°). This gives rise to a grid of interference fringes inside the intercept volume. On the emerging side, three photomultipliers look at this volume under slightly different angles, their average orientation being 15° above the plane of incidence. When droplets cross the intercept volume, the scattered light is modulated in time at a frequency proportional to their velocity. Because of the different orientations of the three photomultipliers, their signals are phase shifted with respect to one another. In the regime of geometrical optics, these phase shifts provide a direct measurement of the diameter of the assumed spherical scatterers[3].

Although this technique is currently applied in fluid mechanics, it is the first time (at our knowledge) that it is used for Helium, i.e. in a situation of a very small contrast of refractive index between the droplets and their environment. We chose a scattering angle of 15°, an unusually low value, in order to guarantee to be in the regime where scattered light comes from refraction through, rather than reflection on, the droplets. We also checked using wave optics calculations and Mie scattering equations[4], that, in our situation, the

geometrical optics formulae usually assumed for the analysis of phase shifts give correct predictions for droplet diameter down to several microns.

In addition, we occasionally tried to visualize the scatterers by imaging the intercept volume into a CCD camera, using the shortest possible frontal focal length (150 mm, as fixed by the distance between the tube and the outer window), resulting in a nominal spatial resolution, as set by the pixel size, of 30 µm.

RESULTS

Starting from a purely stratified flow, with a given total mass rate (6.8 g/s at 1.79K), we gradually turn on the heating power 10 meters upstream from the optical ports, thereby increasing the vapor fraction and its velocity.

Below 40 W (corresponding to a vapor mass rate of 2.1 g/s due to additional heat losses), the scattering of the laser beam is too small to be detected by the naked eye, or by the different photomultipliers (the scattering volume of the PDPA being located at the center of the pipe). Above this value, individual scattering events can be occasionally seen. At 60 W, they occur often enough to give rise to a detectable signal on the central portion of the screen. This is illustrated in FIGURE 2, where we show the background image (due to multiple reflection and stray scattering from the windows), the 60W image, and the contribution of the droplets only, obtained by subtracting these two images. The angular extension of the scattered intensity is sharply limited, due to the digitalization of the video signal. As the heating power is increased, the image becomes brighter and extends in apparent angular size, as the larger vapor velocity drags along a larger liquid fraction. The isotropy of the images in FIGURE 2 shows that the scatterers are not elongated along the flow direction.

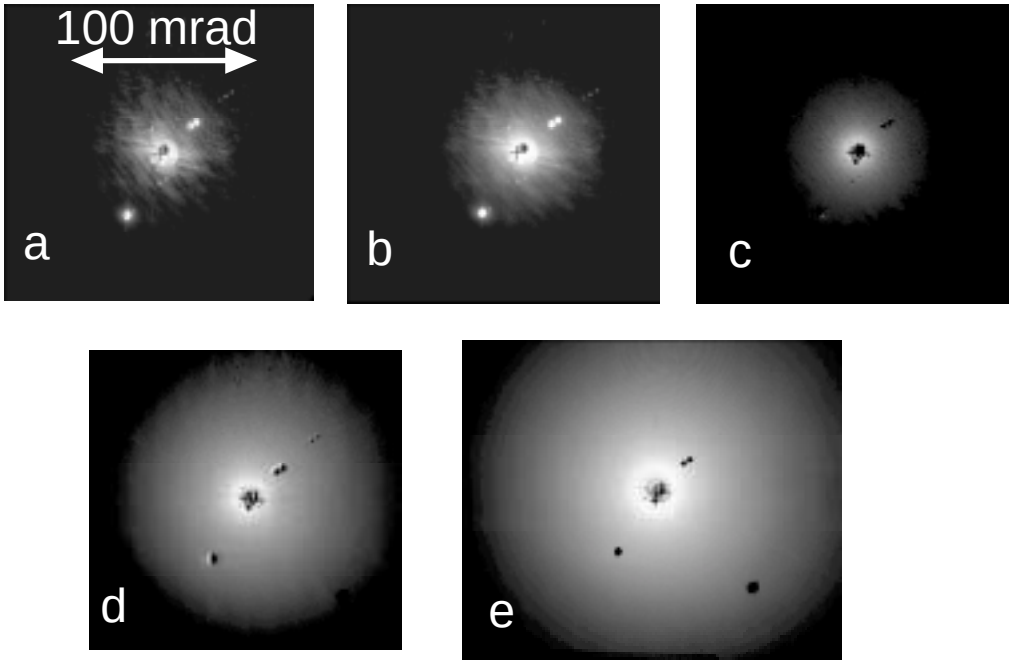

FIGURE 2. pictures of the screen as the heating power is increased (logarithmic gray scale): (a) 0 W (background) ; (b) 60W ; (c), (d), (e) with background subtracted for 60, 86 and 108 W.

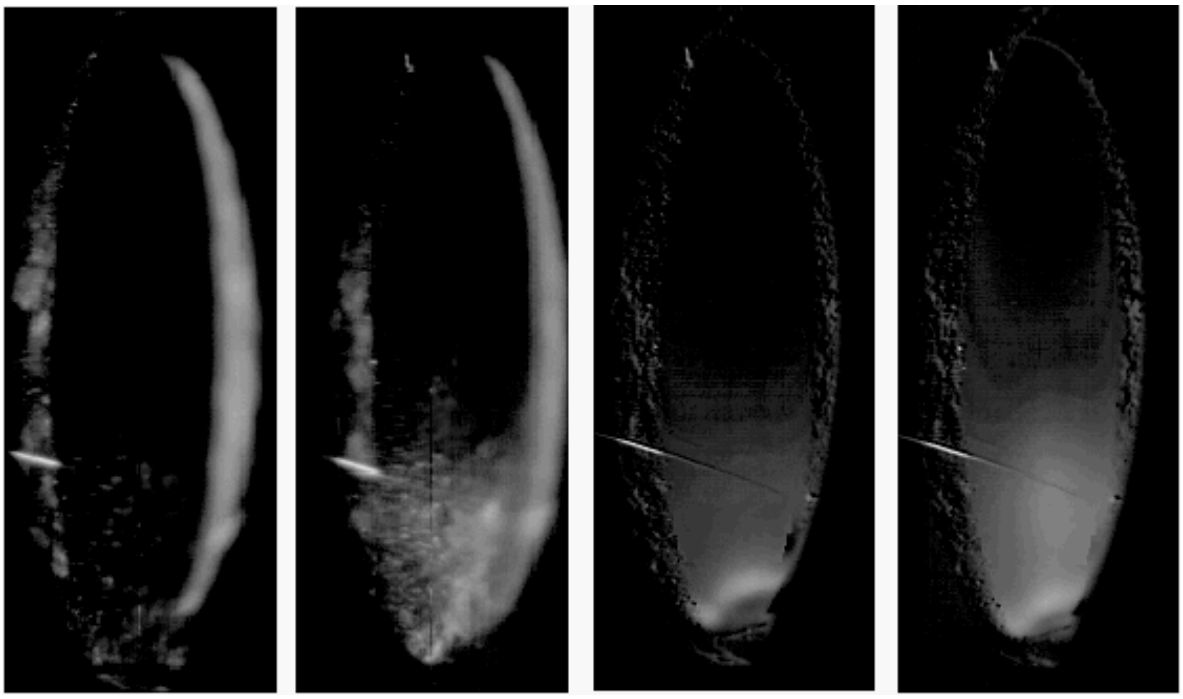

FIGURE 3. From left to right : Snapshots (100 µs) pictures of a slice of the glass tube at 78 W and 109 W and averages of 124 pictures with 40 ms exposure time at 88 and 108W.The snapshot pictures are focused closer to the exit side (left) of the tube, so that droplets close to the other side are blurred. The average interface position appears as the white curved line in the averaged pictures.

Simultaneous snapshot images (100 µs exposure time) of a slice of the glass tube directly show liquid structures inside the vapor phase (FIGURE 3). Note that the extension of the structures is larger than their actual size due to the combination of blurring effects (finite depth of focus) and of the finite droplets velocity (1 mm par 100µs at 10 m/s). Mapping out the height dependence of the signal requires to increase the exposure time, again due to the limited dynamics of the CCD. Typical resulting averaged pictures (with empty tube subtracted) are also shown in FIGURE 3.

ANALYSIS

Size Of Droplets

Let us now turn to a quantitative analysis of the images of FIGURE 2. After due calibration of the measurement chain, the images can be converted into an absolute scattered intensity. By combining images taken with different apertures of the CCD objective, the angular dependence of the scattered intensity can be determined over a large dynamic range.

As shown by FIGURE 4, this dependence is the same for all heating powers (except for 60W, due to the limited dynamic range of the image in this case). Furthermore, for angles larger than 20 mrad, it closely follows the theoretical dependence calculated for spherical scatterers within geometrical optics (for n=1.025). This shows, first, that we are in a single scattering regime (unlike in ref. 2), which is directly checked using the photodiode measurements (we find l>200mm>>L=40mm), and, second, that the spherical droplets must be larger than several microns in diameter.

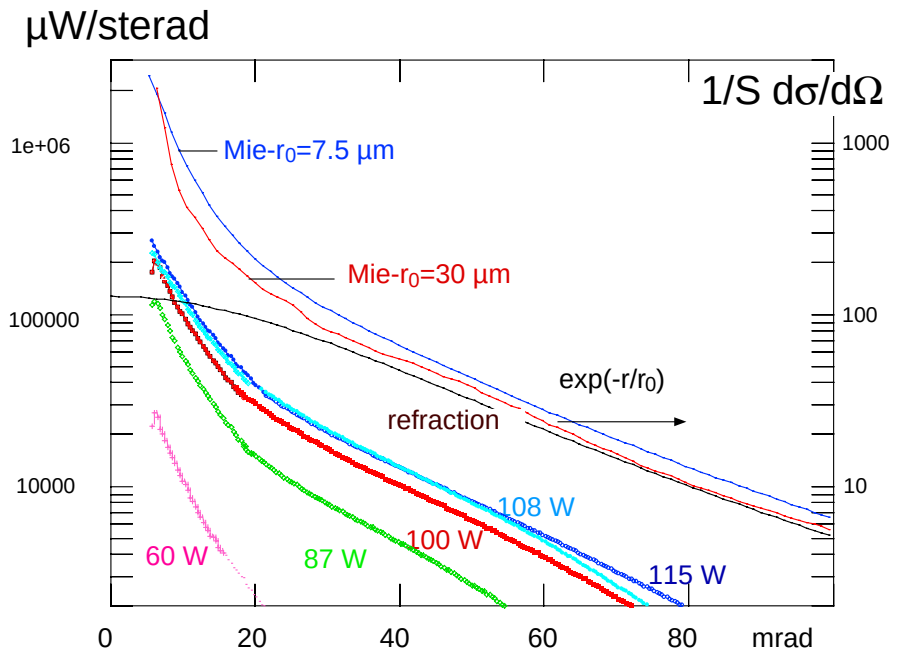

FIGURE 4. The observed angular dependence of the scattered intensity (left scale) is compared to that calculated for spherical scatterers with n=1.025, either in geometrical optics (refraction) or using Mie theory averaged over an exponential distribution of particle radii (right scale, the quantity plotted is the differential scattering cross section, normalized by the geometrical cross section). The two curves shown correspond to average diameters of 15 and 60 µm.

For angles smaller than 20 mrad, we observe a faster increase of the scattered intensity. This is essentially due to diffraction by the large particles. Comparison of our experimental curves to the theory, calculated using the full Mie theory averaged over an exponential distribution of particle radii, suggests that the average diameter of droplets lies in the range of 10-20 µm (see FIGURE 4). This estimation is confirmed by a preliminary analysis of the PDPA results (the PDPA data also show that the detected droplets move essentially at the vapor velocity).

Spatial Distribution Of Mist

For droplets diameters larger than about 10 µm, the scattering cross section is approximately twice the geometrical cross section (equally shared between the refraction and diffraction contributions[4]), i.e. half the droplet area.

This allows us to relate the average mean free path l along a beam path to the interfacial area due to droplets (in mm^2/mm^3) averaged over the same path, according to $1/l=\Sigma/2$. At half tube height, l is obtained from the images in FIGURE 2 (or, directly from the photodiode measurements). A full map of Σ is then obtained from the global images of FIGURE 3, assuming a linear relationship between the brightness of the image and the local interfacial area (we checked that such a relation holds at half tube height, using the laser measurements of Σ above). We show in FIGURE 5 the thus determined profile of Σ along the tube vertical diameter, where we used averaged pictures with different apertures of the CCD objective in order to increase the dynamic range. Beyond the sharp peak, which is due to the liquid-vapor interface, the effect of the droplet mist is clearly seen. As the vapor velocity increases, the droplet density becomes larger, but, remarkably, seems to

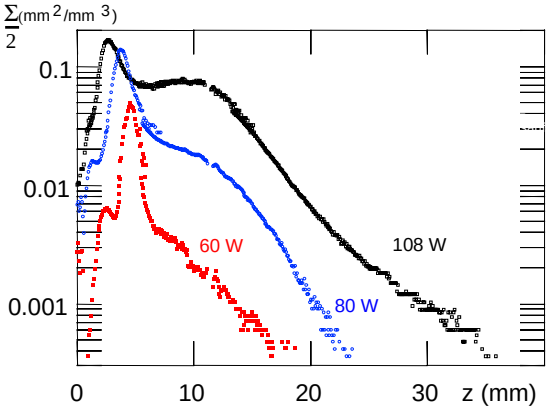

FIGURE 5. Height dependence of the interfacial area, as measured from the images of Fig.3.

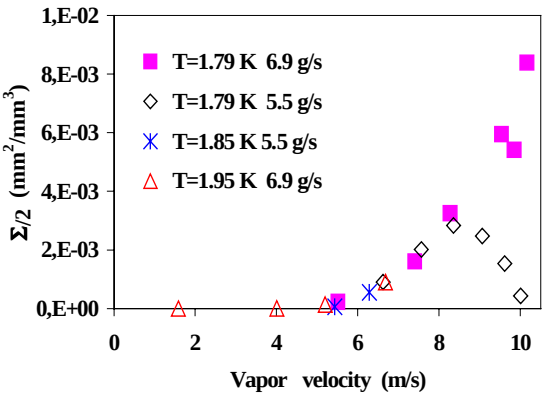

FIGURE 6. Vapor velocity dependence of the interfacial area at tube half height.

fall off exponentially away from the interface, over a nearly constant characteristic distance.

DISCUSSION

FIGURE 6 shows how the interfacial density (as measured with the laser beam) varies with the heating power, for different temperatures -corresponding to different vapor densities- and liquid flow rates. The heating power has been converted into vapor velocity, which makes the different sets of data to approximately collapse on a single curve. This would not be the case, if the power, or the flux of impulsion, were used as abscissa. This may suggest that the velocity is the relevant parameter for atomizing the liquid. Such a dependence has already been found in similar experiments[5]. However, it may seem strange, as one could expect that, at a given vapor velocity, a larger vapor density favors atomization. Namely, in the case where the droplets reach their final size due to shear, the driving parameter should be $\rho_g v_g^2$, where ρ_g and v_g are the vapor density and velocity. Our present results do not seem to corroborate such a picture, as well concerning the lack of density dependence as the final droplets size. In the shear picture, the final diameter d is expected to correspond to a Weber number, We=10, with $We=\rho_g v_g^2 d/\sigma$, where σ is the surface tension. At 1.8 K (ρ_g = 0.46 g/s, σ=3.15 10^{-4} N/m), this corresponds to d= 100 µm for Vg equal to 8 m/s, quite larger than our estimate of 10-20 µm. These discrepancies could perhaps be explained if atomization occurs due to droplets collisions[6]. This is a point we will explore in the future.

Finally, let us give some evaluations for the parameters characterizing the mist. Assuming an average diameter of 20 µm, $\Sigma = 2\ 10^{-2}$ mm^2/mm^3 corresponds to 16 droplets per cubic millimeter. Such droplets cannot be spatially resolved on the pictures of FIGURE 3. On the other hand, a close examination of the snapshots of FIGURE 3, or of high magnification pictures, show the presence of larger particles (100 to 300 µm in diameter) in much smaller number. It is presently not clear whether these large particles are clouds of the smaller droplets above, or whether they are true, rare, large droplets and, in this case, whether they contribute significantly to the flow of dispersed liquid. Assuming that only the small droplets contribute, and that their radial velocity v_r is of order of the fluctuations of the axial velocity measured by the PDPA (about 1 m/s), the volume flow

rate incident on the walls (per unit area) is $\Sigma\, d/2\, v_r /3$. Per cm length of the tube, we thus estimate a typical flow rate of order 100 mm^3/s, corresponding to 300 mW of cooling power. For the Kapitza box described in ref. 1 (length 40 cm), the maximal cooling power provided by this flow is 12 W. This is only one order of magnitude larger than the power beyond which the heat removal seems to decrease, which is not inconsistent with the idea that the droplet mist could be the mechanism for the extra exchange we observe.

CONCLUSION

By using optical techniques, we have confirmed, that at high vapor velocity, the expectation that mist flow should occur. A thorough analysis of the results will allow complete characterization of the mist, and to evaluate its possible effect on the heat transfer.

REFERENCES

1. Rousset B**.** and al., "HeII Co-Current Two Phase Flow At High Vapor Velocities " *to be published in the proceeding of this conference*
2. Ladam Y. and al., "Light Scattering by a Liquid-Gas Helium Spray " *to be published in European Journal of physics (Applied Physics) 2001*
3. Bachalo W. D., "Development of The Phase/doppler Spray Analyser for Liquid Drop size and Velocity Characterizations" *Proc.AIAA/SAE/ASME 20th Joint Propulsion Conference*, Cincinati, Ohio (1984)
4. Van de Hulst H. C., "Light Scattering by small particles" *John Wiley & Sons, New York* (1957) (*Dover paperback reprint, 1981)*
5. Ishii M. and Grolmes M.A., "Inception Criteria for Droplet Entrainment in Two-phase Concurrent Film Flow" *AIChE Journal* (1975), Vol. 21, 308-318
6. Hopfinger E., *private communication*